Heme Reduction by Intramolecular Electron Transfer in Cysteine Mutant Myoglobin under Carbon Monoxide Atmosphere†

Shun Hirota,*,‡,§ Kayo Azuma,‡ Makoto Fukuba,‡ Shigeki Kuroiwa,‡ and Noriaki Funasaki‡

Department of Physical Chemistry, 21st Century COE Program, Kyoto Pharmaceutical University, 5 Nakauchi-cho, Misasagi, Yamashina-ku, Kyoto 607-8414, Japan, and PRESTO, Japan Science and Technology Agency, Kawaguchi, Saitama 332-0012, Japan

Received April 26, 2005; Revised Manuscript Received June 13, 2005

ABSTRACT: Human myoglobin (Mb) possesses a unique cysteine (Cys110), whereas other mammalian Mbs do not. To investigate the effect of a cysteine residue on Mb, we introduced cysteine to various sites on the surface of sperm whale Mb (K56C, V66C, K96C, K102C, A125C, and A144C) by mutation. The cysteines were inserted near the end of α-helices, except for V66C, where the cysteine was introduced in the middle of an α-helix. Reduction of the heme was observed for each mutant *met*Mb by incubation at 37 °C under carbon monoxide atmosphere, which was much faster than reduction of wild-type *met*Mb under the same condition. Heme reduction did not occur significantly under nitrogen or oxygen atmospheres. The rate constant for heme reduction increased for higher mutant Mb concentration, whereas it did not change significantly when the CO concentration was reduced from 100% CO to 50% CO with 50% O_2. The similarity in the rate constants with different CO concentrations indicates that CO stabilizes the reduced heme by coordination to the heme iron. SDS−PAGE analysis showed that mutant Mb dimers were formed by incubation under CO atmosphere but not under air. These dimers were converted back to Mb monomers by an addition of 2-mercaptoethanol, which showed formation of a Mb dimer through a disulfide bond. The rate constant decreased in general as the heme−cysteine distance was increased, although V66C Mb exhibited a very small rate constant. Since V66 is placed in the middle of an α-helix, steric hindrance would occur and prevent formation of a dimer when the cysteine residues of two different V66C Mb molecules interact with each other. The rate constants also decreased for K56C and A144C Mbs presumably because of the electrostatic repulsion during dimer formation, since they are relatively charged around the inserted cysteine.

The knowledge of the importance of cysteine for protein structure and reaction has been increasing. Cysteine serves as the proximal axial ligand for the heme in O_2 activating heme proteins, such as cytochrome P450 and nitric oxide synthase (*1*). It has been proposed that the cysteinate ligand of P450 plays a key mechanistic role as a strong internal electron donor to promote O−O bond cleavage in the ferric−peroxide intermediate and to generate the high oxidation ferryl−oxo state of the reaction cycle (*2*, *3*). The aerobic class Ia ribonucleotide reductase of *Escherichia coli* is composed of two homodimeric components, proteins R1 and R2, and the early radical intermediate of protein R1 has been postulated to be a cysteinyl radical, which is in close proximity to the diiron−oxo site (*4*).

Oxidation of two cysteines in close proximity with each other would favor the formation of a disulfide bond, which is hydrophobic and often vital for the folding, stability, and reaction of the protein. The disulfide bond stabilizes the protein by reducing the entropy of the denatured state, together with enthalpic and native state effects (*5*). Cleavage of one or more of the disulfide bonds controls the function of some secreted soluble proteins and cell surface receptors (*6*). In neuroglobin, a newly found dioxygen binding protein, two cysteines are sufficiently close to form an internal disulfide bond, where reduction of the disulfide bond decreases its oxygen affinity (*7*). Cysteine-modified structures have been reported in several metalloenzymes. For example, the two cysteine residues coordinated to the iron were posttranslationally modified to cysteine-sulfenic and -sulfinic acids in iron-containing nitrile hydratase, which catalyzes the hydration of nitriles to their corresponding amides (*8*). The sulfur atom of a cysteine residue was intrachain cross-linked to an orthoquinone-modified tryptophan in amine dehydrogenase (AMDH),[1] which converts amine into cor-

† This work was partially supported by Grants-in-Aid for Scientific Research from the Ministry of Education, Culture, Sports, Science, and Technology of Japan (Priority Areas, Water and Biomolecules, No. 164041242, S.H.), the 21st COE Program (S.H.), the Japan Society for Promotion of Science (Category C, No. 16550149, S.H.), the Japan Science and Technology Agency, the Shimadzu Science Foundation, the Takeda Science Foundation, and the Mitsubishi Chemical Corporation Fund.

* To whom correspondence should be addressed at Kyoto Pharmaceutical University. Tel: +81-75-595-4664. Fax: +81-75-595-4762. E-mail: hirota@mb.kyoto-phu.ac.jp.

‡ Kyoto Pharmaceutical University.

§ PRESTO, Japan Science and Technology Agency.

[1] Abbreviations: Mb, myoglobin; AMDH, amine dehydrogenase; cyt *c*, cytochrome *c*; PFe-Ru, pentaammineruthenium(His33)cytochrome *c*; bpy, 2,2′-bipyridine; im, imidazole; SDS−PAGE, sodium dodecyl sulfate−polyacrylamide gel electrophoresis; DMPO, 5,5-dimethylpyrroline *N*-oxide.

10.1021/bi0507581 CCC: $30.25
Published on Web 07/09/2005

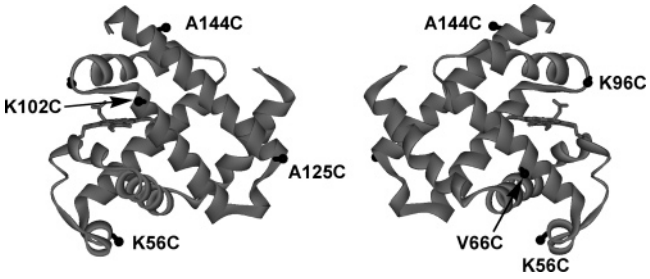

FIGURE 1: Structure of sperm whale Mb (PDB entry 1DUK) from opposite directions. Amino acids modified to cysteine in this study are shown in black spots.

responding aldehydes (*9*, *10*). Additional cross-links were also detected in AMDH, where a cysteine side chain was bridged to a carboxylic acid side chain of an aspartate or a glutamate residue (*9*, *10*). We have also found modification of Ni-coordinating cysteines at the active site of [NiFe] hydrogenase (*11*).

Myoglobin (Mb) is a well-known heme protein, which consists of 153 amino acids with eight α-helices and seven nonhelical segments (Figure 1) (*12*, *13*). The heme is coordinated by a histidine nitrogen, and the oxygen binds to the heme iron in the opposite position of this histidine. Human Mb possesses a unique cysteine at position 110 (Cys110), while other mammalian Mbs do not have any cysteine (*14*). It has been shown that an addition of hydrogen peroxide to human Mb generates Trp14-peroxyl, Tyr103-phenoxyl, and Cys110-thiyl radicals and coupling of Cys110-thiyl radical yields a homodimer through intermolecular disulfide bond formation (*15*). There have been several studies on the reduction of Mb. For example, dihydrolipoic acid is reported to reduce *met*Mb to oxyMb (*16*), whereas glutathione and ergothioneine can reduce the ferryl state of Mb to *met*Mb (*17*, *18*), although it cannot reduce *met*Mb further.

Electron transfer processes in proteins are key steps in biological functions, such as photosynthesis and respiration (*19*). Much has been learned about the mechanism of electron transfer of proteins with the use of small metalloproteins and small inorganic complexes. Several methods have been applied to elucidate the spatial relationship between the donor and acceptor in a biomolecule and to define the intramolecular electron transfer rates. Particularly, photochemical methods have been applied to study intramolecular electron transfer in hemoproteins (*20*). Synthesized porphyrins were incorporated into the protein matrix of myoglobin (Mb) to construct a photochemical system (*21*−*24*), whereas protohemin molecules with $Ru(bpy)_3$ have been synthesized and incorporated into the heme crevice of Mb (*23*, *24*). Gray and co-workers have utilized Ru-modified metalloproteins in an elegant way to study intramolecular electron transfer reaction rates between redox centers in proteins (*25*, *26*). Electron transfer in a Ru-modified protein was first reported with a pentaammineruthenium(III)(His33)ferricytochrome *c* (PFe^{III}-Ru^{III}), where the redox centers, the heme and modified His33, were separated by 15 Å (*27*, *28*). Electron transfer from electronically excited $Ru(bpy)_3^{2+}$ to PFe^{III}-Ru^{III} produced PFe^{III}-Ru^{II} in 5-fold excess to PFe^{II}-Ru^{III}, where PFe^{III}-Ru^{II} decayed to PFe^{II}-Ru^{III} by intramolecular electron transfer.

To investigate the effect of the cysteine residue in Mb and also to obtain insights into the cysteine oxidation process in proteins, we introduced cysteine to various positions on the surface of sperm whale Mb (Figure 1). We found that intramolecular electron transfer from the cysteine to the heme occurs within the protein in mutant *met*Mbs under carbon monoxide atmosphere, producing a Mb dimer with a disulfide bond.

Table 1: Nucleotide Sequences of the Primers

primer	sequence[a]
pEMBL-F1	CGGATAACAATTTCACACAGG
pEMBL-R1	TAACGCCAGGGTTTTCCCA
pK56C-F1	AGCTGAAATGTGCGCTTCTGAAG
pK56C-R1	CTTCAGAAGCGCACATTTCAGCT
pV66C-F1	AAACATGGTTGCACCGTGTTAAC
pV66C-R1	GTTAACACGGTGCAACCATGTTT
pK96C-F1	GCATGCTACTTGCCATAAGATCC
pK96C-R1	GGATCTTATGGCAAGTAGCATGC
pK102C-F1	GATCCCGATCTGCTACCTGGAAT
pK102C-R1	ATTCCAGGTAGCAGATCGGGATC
pA125C-F1	TAACTTCGGTTGCGACGCTCAGG
pA125C-R1	CCTGAGCGTCGCAACCGAAGTTA
pA144C-F1	GATATCGCTTGCAAGTACAAAGAAC
pA144C-R1	GTTCTTTGTACTTGCAAGCGATATC

[a] Underlines indicate the nucleotides for the modified amino acid.

MATERIALS AND METHODS

Site-Directed Mutagenesis and Protein Purification. Enzymes for site-directed mutagenesis were obtained from Takara Shuzo Co. (Kyoto, Japan). Oligonucleotide primers were purchased from Kurabo Industries Ltd. (Osaka, Japan). Amino acid substitutions of sperm whale Mb at the Lys56, Val66, Lys96, Lys102, Ala125, and Ala144 positions were introduced by PCR-based in vitro mutagenesis of a Mb expression vector as follows (*29*): Using a pMb413a-derived plasmid which carried the cDNA of the sperm whale precursor Mb as a template (*30*, *31*), two DNA segments were initially amplified with pEMBL-F1 and pXX-R1 (Table 1) primers and pEMBL-R1 and pXX-F1 (Table 1) primers, respectively, and then purified. The overlap region of the two PCR products was successively extended by an additional PCR with pEMBL-F1 and pEMBL-R1 primers. The resulting PCR product, which contained the full-length cDNA of the mutant sperm whale precursor Mb, was digested with *Pst*I and *Kpn*I and inserted into the *Pst*I−*Kpn*I site of the pMb413a expression vector. The obtained plasmids were introduced into *E. coli* TB-1 using a competent cell. Plasmid DNAs were prepared using an Accuprep plasmid extraction kit (Bioneer, City, South Korea). DNA sequencing was carried out with a BigDye Terminator v1.1 cycle sequencing kit (Applied Biosystems, Inc., City, CA) and an ABI PRISM 310 genetic analyzer sequencing system (Applied Biosystems, Inc.).

Recombinant sperm whale Mb was overproduced in *E. coli* TB-1 cells. *Met*Mb was purified by the reported method (*32*) with a few modifications. Dithiothreitol (2 mM) was added during extraction of Mb from the cells. The extracted Mb solution was added with hemin (0.1 mM) and stirred for 30 min at 4 °C. After purification with a DEAE column, Mb was completely oxidized with a small amount of potassium ferricyanide dissolved in the buffer and purified with a CM-52 column (Whatman). We washed Mb with buffer thoroughly during purification with the CM column to avoid the effect of ferricyanide introduced and ferrocya-

nide, which may be produced. Removal of ferrocyanide was confirmed by comparison of the difference absorption spectra of Mb observed during the heme reduction with the difference spectrum between ferricyanide and ferrocyanide. Purified *met*Mb was dialyzed with 10 mM potassium phosphate buffer, pH 7.0, before each measurement. The absorption spectra of mutant Mbs were identical with the spectrum of wild-type Mb, which showed no significant perturbation on the Mb structure by the mutation. The purity of each protein was confirmed by the SDS−PAGE analysis and by the absorbance (Abs) ratio between 280 and 409 nm ($Abs_{409}/Abs_{280} > 4.6$). The concentration of the protein was adjusted by the absorption spectrum.

Spectroscopic Measurements. The absorption change of sperm whale *met*Mb at 37 °C was recorded on a Shimadzu UV-3100PC spectrophotometer. *Met*Mb (2−18 μM) in 10 mM potassium phosphate buffer, pH 6.0 or 7.0, was transferred into a quartz cell. To obtain N_2 atmosphere, the cell was degassed and refilled with N_2 using a vacuum line. For introduction of CO, the cell was first filled with N_2, then degassed, and refilled with CO. First-order reaction rate constants k_{obs} of the heme reduction were obtained from the slopes of the absorption changes. The actual rates for the heme reduction of mutant *met*Mbs by the cysteine residues were estimated by subtracting the effect of direct heme reduction by CO.

SDS−PAGE Analysis of MetMb. Mutant sperm whale *met*Mb in 10 mM potassium phosphate buffer, pH 7.0, was placed under air or CO atmosphere at 37 °C for 15 h. For reduction of disulfide bonds, *met*Mb was incubated with 2-mercaptoethanol (2% v/v) at 90 °C for 5 min after treatment with CO. Sodium dodecyl sulfate−polyacrylamide gel electrophoresis (SDS−PAGE) analysis was performed for each sample using a 15% separation gel without 2-mercaptoethanol. The obtained gel was stained with CBB R-250.

RESULTS

Heme Reduction of Cysteine-Introduced MetMb. The Soret band of mutant sperm whale *met*Mb at pH 7.0 was detected at 409 nm, which showed that the heme structure was not perturbed significantly by cysteine mutation. By incubation at 37 °C under CO atmosphere, the Soret band of K96C gradually was red shifted, and new bands were generated at about 542 and 580 nm (Figure 2A). These changes are clearly seen by calculating the difference spectra with the initial spectra (Figure 2B). Isosbestic points were observed at about 345, 416, 462, and 524 nm in the difference spectra, which demonstrated that no stable intermediate was generated at the heme site during the reduction. The same changes were observed in the absorption spectra of other cysteine-introduced mutant *met*Mbs by incubation under CO atmosphere. These changes are typical for generation of CO-bound Mb, which shows that the heme of cysteine mutant Mbs is reduced by incubation with CO. The absorption spectra of mutant *met*Mbs, however, changed little under nitrogen or oxygen atmosphere.

Since CO-driven reduction has been reported for cytochrome *c* oxidase ($CO + 2OH^- \rightarrow CO_2 + H_2O + 2e^-$) (*33*, *34*), one may claim that sperm whale Mb could also be reduced slowly at 37 °C under CO atmosphere, although its redox potential is relatively low. Actually, wild-type sperm whale *met*Mb was reduced very slowly at 37 °C under CO atmosphere, but the rate was significantly slower than the rates of cysteine mutant *met*Mbs, more than an order of magnitude slower except for V66C Mb (see text below). The difference in the reduction rates suggests that the heme of mutant *met*Mbs was reduced by a different reducing agent than CO, probably the introduced cysteine residue. The actual rate constants (k_{obs}) for the heme reduction of mutant *met*Mbs by the cysteine residues were estimated by subtracting the effect of direct heme reduction by CO determined from the reduction of wild-type Mb by CO under the same condition. The absorption changes of mutant Mbs were less than 0.001 at 310 nm (absorption minimum for oxidized Mb), while a larger absorption difference (about 0.008) was detected in the difference spectrum between 5 μM ferricyanide and ferrocyanide at 310 nm. The results showed that the heme was not reduced by ferrocyanide, which may be produced during the Mb oxidation process.

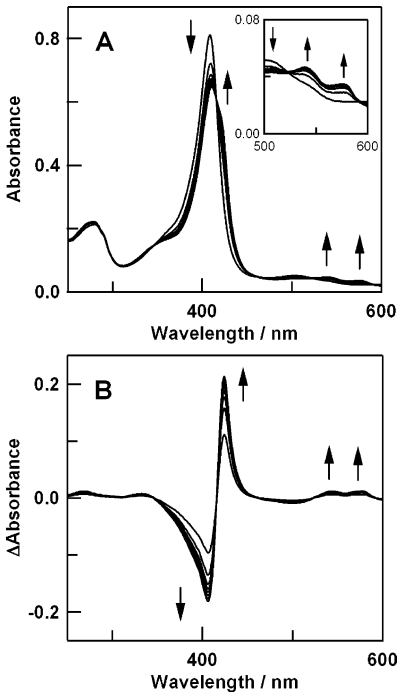

FIGURE 2: Change in the absorption spectra of K96C *met*Mb under CO atmosphere: (A) absorption spectra and (B) difference absorption spectra between the initial absorption spectrum. Inset: Enlarged view of the absorption spectra in the 500−600 nm region. The spectra were taken at the beginning of the reaction and then after each hour for 8 h. Experimental conditions: Mb, 5 μM; phosphate buffer, 10 mM; pH 7.0; 37 °C.

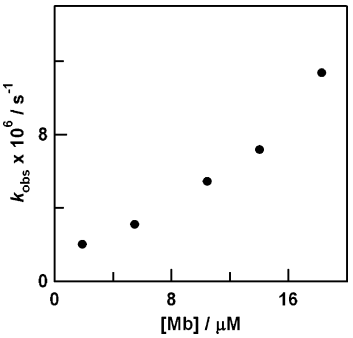

FIGURE 3: Plots of k_{obs} vs protein concentration of K102C Mb under CO atmosphere. Other experimental conditions are the same as those used in Figure 2.

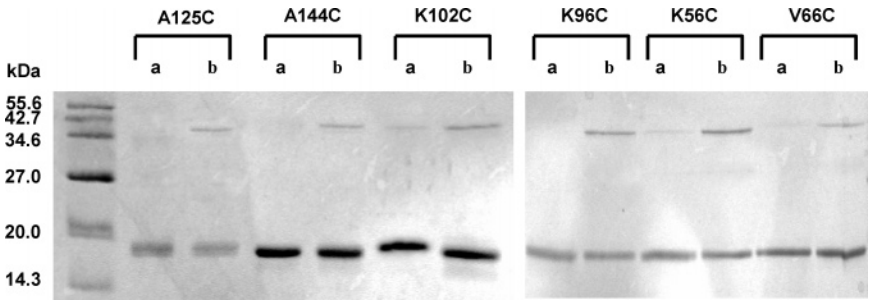

FIGURE 4: SDS−PAGE analysis of cysteine-introduced *met*Mbs incubated under (a) air and (b) CO atmosphere. *Met*Mbs were incubated at 37 °C for 15 h in phosphate buffer (10 mM), pH 7.0.

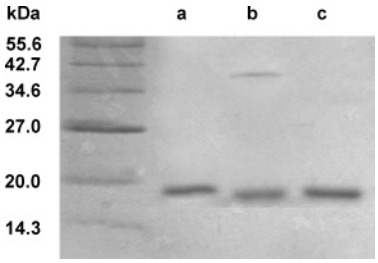

FIGURE 5: SDS−PAGE analysis of K56C *met*Mb after incubation under (a) air and (b, c) CO atmosphere: (b) untreated and (c) treated with 2-mercaptoethanol before analysis. Experimental conditions were the same as those used in Figure 4.

The reduction rate constant k_{obs} of K102C Mb increased with increasing the Mb concentration from 2 to 18 μM (Figure 3), which suggested intermolecular interaction during the reaction. When the CO concentration was reduced from 100% CO to 50% CO with 50% O_2, no significant change was observed in the reduction rate for mutant Mbs, while the rate constant decreased for wild-type Mb. The similarity in the rate constants under different CO concentrations for mutant Mbs indicates that CO stabilizes the reduced heme by coordination to the heme iron. With decreasing the pH from 7.0 to 6.0 and an addition of 100 mM NaCl, the rate constant decreased to about 50% and 30−50%, respectively, whereas the rate constant for wild-type Mb did not change significantly.

Dimerization of Mb. Each mutant *met*Mb was incubated at 37 °C under air and subsequently subjected to SDS−PAGE analysis without 2-mercaptoethanol. Mutant Mbs incubated under air exhibited bands at a molecular weight of about 18 000, which corresponded to that of Mbs (Figure 4a). For the mutant Mb solutions incubated under CO atmosphere, the dimer peaks at a molecular weight of 36 000 emerged, whereas the intensities of the monomer bands were not perturbed significantly (Figure 4b). For the protein solutions obtained by the reaction under CO atmosphere with 100 mM NaCl, the intensities of the dimer bands in the SDS−PAGE analysis decreased significantly. The weaker dimer band is consistent with the decrease in the rate constant by an addition of NaCl (see text above).

The dimer bands of the CO-treated samples disappeared by incubation with 2-mercaptoethanol (Figure 5). The results show that Mb dimers were formed through an intermolecular S−S bond of their introduced cysteines, and the disulfide bond can be produced under CO but not without CO.

DISCUSSION

Heme Reduction and Dimerization of Cysteine-Introduced Mb. The reduction of the heme of cysteine mutant Mbs may be due to electron transfer from the cysteine thiolate, deprotonated cysteine sulfur atom, to the heme. The thiolate species would be produced in a certain amount at pH 7, since the pK_a for the cysteine thiol is 8.37. The amount of the thiolate species and the rate of heme reduction would depend on pH. However, there is an effect of the heme axial exchange from water to hydroxide with increasing the pH, and thus we investigated the effect of lowering the pH. The rate of the heme reduction for the mutant Mbs was decreased by decreasing the pH from 7.0 to 6.0, which supports electron transfer from the thiolate species. The electron transfer rate was also decreased by an addition of 100 mM NaCl, which may be attributed to stabilization of the thiolate species by interaction with Na^+.

By an addition of 100 mM NaCl, the intensities of the dimer bands of the reaction solution in the SDS−PAGE analysis were decreased significantly. The heme reduction rate of cysteine mutant Mb increased for higher protein concentration (Figure 3). These results are consistent with the interpretation that dimerization of cysteine mutant Mb occurs during the reduction of the heme. Dimerization occurs through an intermolecular S−S bond, which suggests formation of cysteinyl radicals by electron transfer from the cysteine to the heme. The cysteinyl radical, however, must have been produced very slowly, since the reduction of the heme in mutant Mb was very slow, although the radical may react very rapidly with the cysteine thiol group of another Mb molecule to form a Mb dimer. Actually, the cysteinyl radical was not detectable by EPR measurements even by using a spin-trap reagent, 5,5-dimethylpyrroline *N*-oxide (DMPO).

A similar dimerization reaction has been observed by an addition of hydrogen peroxide to human Mb (*15*), which possesses a unique Cys110, and dimerization occurred by coupling of the produced Cys110-thiyl radicals (*14*). Cys110 is located on the protein surface of human Mb (*14*), and the protein forms a disulfide bond by reaction with H_2O_2 (*15*). The present results in cysteine mutant Mb suggest that CO may react with human *met*Mb and reduce the heme, where the heme could receive an electron from the cysteine residue.

Factors Controlling the Rate of Heme Reduction. To investigate the effect of the heme−Cys distance on the heme reduction rate, the distance for each mutant was defined as the shortest distance between the heme macrocycle and the β-carbon of the original amino acid that was modified to cysteine. The rate constant k_{obs} decreased in general as the heme−Cys distance was increased, although V66C Mb exhibited a significantly small k_{obs} value (see text below).

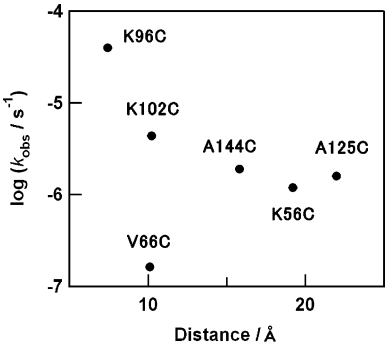

FIGURE 6: Correlation between log k_{obs} and the heme−Cys distance for mutant Mbs. Experimental conditions (for all mutant Mbs): protein concentration, 5 μM; phosphate buffer, 10 mM; pH 7.0; 37 °C.

Theoretical studies have shown that the electronic coupling strength decays exponentially with increasing donor−acceptor separation. In the case of Ru-modified metalloproteins, the reduction depended on the donor−acceptor distance, although the medium separating two redox sites in a protein is a heterogeneous array of bonded and nonbonded interactions (*35*, *36*). For $Ru(bpy)_2(imidazole)^{2+}$-modified azurins, variation of the electron transfer rate constant with direct metal−metal separation was well described by an exponential function (*37*). The rate constants for the heme reduction of mutant Mbs in this study are thus plotted for the logarithm of k_{obs} versus the heme−Cys distance (Figure 6).

The value of log k_{obs} decreased in general as the heme−Cys distance was increased. The effect of the heme−Cys distance on log k_{obs} was more significant when the heme−Cys distance was shorter (Figure 6). The reduction rate of V66C Mb, however, was much slower than that of K102C Mb, although the heme−Cys distances are about the same for these mutants (Figure 6). V66C is placed in the middle of an α-helix, whereas cysteines of other mutant Mbs including K102C Mb are introduced near the end of α-helices. Steric hindrance, therefore, would occur during formation of V66C Mb dimers, which prevents dimer formation and reduction of the heme, while other mutant Mbs do not suffer significant steric hindrance during dimer formation. In the SDS−PAGE analysis of V66C Mb by incubation under CO atmosphere, the intensity of the band attributed to the dimer was relatively weak compared to the dimer peaks of other mutant Mbs (Figure 3), which demonstrated the difficulties in dimerization and heme reduction for this mutant. These results show that the intermolecular interaction is an important factor for the reaction. The heme reduction rate of cysteine-introduced mutant Mb increased for higher Mb concentration (Figure 4), which showed that reduction of the heme by the cysteine residue in mutant Mb is affected by intermolecular interaction. The slope in Figure 6 was significantly smaller than that obtained for electron transfer in proteins (*25*, *26*), since there was a significant effect by dimerization in cysteine mutant Mb.

The rate constants of heme reduction for K56C and A144C Mbs exhibited smaller values compared with those estimated from a linear correlation between the logarithm of the rate constants and the heme−Cys distances for K102C and A125C Mbs (Figure 6). Since positively charged lysine residues are distributed around the inserted Cys for A144C Mb, the lysine residues may cause intermolecular repulsion between the Cys sites of different Mb molecules and inhibit formation of A144C Mb dimers. The positive charges may also stabilize the deprotonated negatively charged S^- of the cysteine residue and inhibit intramolecular electron transfer for this mutant. For K56C Mb, negatively charged amino acids, glutamic acid and aspartic acid residues, are distributed around the introduced cysteine, and the negatively charged amino acids around the cysteine may also cause repulsion during dimerization. These results support the conclusion that the ability of dimerization may control intramolecular electron transfer and reduction of the heme.

The heme−Cys distance of human Mb is about 10 Å, as judged from the crystal structure of its C110A mutant (PDB entry 2MM1). This distance is comparable to the heme−Cys distances for K102C and V66C sperm whale Mbs. Cys110 of human Mb, however, is placed in the middle of an α-helix, which is comparable to the position of the inserted Cys in V66C sperm whale Mb. Therefore, reduction of the heme in human Mb would not be very significant, although it may occur.

Mechanism of Heme Reduction and Mb Dimerization. Absorption measurements showed that heme reduction occurred by incubation under CO atmosphere, but little under oxygen or nitrogen atmosphere. Similarly, the SDS−PAGE analysis showed that Mb dimers with intermolecular S−S bonds were produced only by incubation under CO atmosphere. We interpret that the heme of Mb is reduced by the cysteine thiolate in cysteine-introduced Mbs, and as a result a cysteinyl radical is produced (Figure 7). $Mb(Fe^{III})$/Cys and the electron transfer product, $Mb(Fe^{II})$/$Cys^{\bullet}$, may form an equilibrium, which is usually shifted to the left. Since CO binds strongly to the reduced heme, reduction of the heme is enhanced by an addition of CO. As a result, the equilibrium is shifted to the right and a cysteinyl radical may generate. When the cysteinyl radical produced reacts with another cysteinyl radical of a different Mb molecule, a Mb dimer may form through an intermolecular S−S bond, whereas the heme is kept reduced with the bound CO.

The present work shows that a cysteine residue in the protein may reduce the heme of *met*Mb by functioning as an electron donor site. The rate of heme reduction is affected not only by the heme−Cys distance but also by the capability to form a dimer with a S−S bond. Similar electron transfer from a cysteine to a metal site may occur in other metalloproteins.

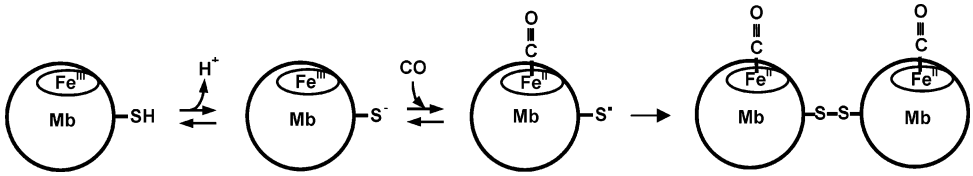

FIGURE 7: Schematic view of reduction and dimerization of the cysteine mutant Mb under CO atmosphere.

ACKNOWLEDGMENT

We thank Professor John S. Olson (Rice University) for a kind gift of sperm whale Mb plasmid and Dr. Makoto Nagaoka (Kyoto Pharmaceutical University) for help in mutant Mb preparation.

REFERENCES

1. Sono, M., Roach, M. P., Coulter, E. D., and Dawson, J. H. (1996) Heme-containing oxygenases, *Chem. Rev. 96*, 2841−2888.
2. Dawson, J. H. (1988) Probing structure−function relations in heme-containing oxygenases and peroxidases, *Science 240*, 433−439.
3. Liu, H. I., Sono, M., Kadkhodayan, S., Hager, L. P., Hedman, B., Hodgson, K. O., and Dawson, J. H. (1995) X-ray absorption near edge studies of cytochrome P-450-CAM, chloroperoxidase, and myoglobin. Direct evidence for the electron releasing character of a cysteine thiolate proximal ligand, *J. Biol. Chem. 270*, 10544−10550.
4. Persson, A. L., Sahlin, M., and Sjöberg, B.-M. (1998) Cysteinyl and substrate radical formation in active site mutant E441Q of *Escherichia coli* class I ribonucleotide reductase, *J. Biol. Chem. 273*, 31016−31020.
5. Betz, S. F. (1993) Disulfide bonds and the stability of globular proteins, *Protein Sci. 2*, 1551−1558.
6. Hogg, P. J. (2003) Disulfide bonds as switches for protein function, *Trends Biochem. Sci. 28*, 210−214.
7. Hamdane, D., Kiger, L., Dewilde, S., Green, B. N., Pesce, A., Uzan, J., Burmester, T., Hankeln, T., Bolognesi, M., Moens, L., and Marden, M. C. (2003) The redox state of the cell regulates the ligand binding affinity of human neuroglobin and cytoglobin, *J. Biol. Chem. 278*, 51713−51721.
8. Nagashima, S., Nakasako, M., Dohmae, N., Tsujimura, M., Takio, K., Odaka, M., Yohda, M., Kamiya, N., and Endo, I. (1998) Novel non-heme iron center of nitrile hydratase with a claw setting of oxygen atoms, *Nat. Struct. Biol. 5*, 347−351.
9. Vandenberghe, I., Kim, J.-K., Devreese, B., Hacisalihoglu, A., Iwabuki, H., Okajima, T., Kuroda, S., Adachi, O., Jongejan, J. A., Duine, J. A., Tanizawa, K., and Beeumen, J. V. (2001) The covalent structure of the small subunit from *Pseudomonas putida* amine dehydrogenase reveals the presence of three novel types of internal cross-linkages, all involving cysteine in a thioether bond, *J. Biol. Chem. 276*, 42923−42931.
10. Datta, S., Mori, Y., Takagi, K., Kawaguchi, K., Chen, Z.-W., Okajima, T., Kuroda, S., Ikeda, T., Kano, K., Tanizawa, K., and Mathews, F. S. (2001) Structure of a quinohemoprotein amine dehydrogenase with an uncommon redox cofactor and highly unusual crosslinking, *Proc. Natl. Acad. Sci. U.S.A. 98*, 14268−14273.
11. Ogata, H., Mizoguchi, Y., Mizuno, N., Miki, K., Adachi, S., Yasuoka, N., Yagi, T., Yamauchi, O., Hirota, S., and Higuchi, Y. (2002) Structural and spectroscopic studies of the carbon monoxide complex of [NiFe]hydrogenase from *Desulfovibrio vulgaris* Miyazaki F: Suggestion for the initial activation site for dihydrogen, *J. Am. Chem. Soc. 124*, 11628−11635.
12. Kendrew, J. C., Dickerson, R. E., Strandberg, B. E., Hart, R. G., Davies, D. R., Phillips, D. C., and Shore, V. C. (1960) Structure of myoglobin. A three-dimensional Fourier synthesis at 2 Å resolution, *Nature 185*, 422−427.
13. Phillips, S. E. V. (1978) Structure of oxymyoglobin, *Nature 273*, 247−248.
14. Hubbard, S. R., Hendrickson, W. A., Lambright, D. G., and Boxer, S. G. (1990) X-ray crystal structure of a recombinant human myoglobin mutant at 2.8 Å resolution, *J. Mol. Biol. 213*, 215−218.
15. Witting, P. K., Douglas, D. J., and Mauk, A. G. (2000) Reaction of human myoglobin and H_2O_2. Involvement of a thiyl radical produced at cysteine 110, *J. Biol. Chem. 275*, 20391−20398.
16. Romero, F. J., Ordonez, I., Arduini, A., and Cadenas, E. (1992) The reactivity of thiols and disulfides with different redox states of myoglobin. Redox and addition reactions and formation of thiyl radical intermediates, *J. Biol. Chem. 267*, 1680−1688.
17. Galaris, D., Cadenas, E., and Hochstein, P. (1989) Glutathione-dependent reduction of peroxides during ferryl- and met-myoglobin interconversion: A potential protective mechanism in muscle, *Free Radical Biol. Med. 6*, 473−478.
18. Arduini, A., Eddy, L., and Hochstein, P. (1990) The reduction of ferryl myoglobin by ergothioneine: A novel function for ergothioneine, *Arch. Biochem. Biophys. 281*, 41−43.
19. Berg, J. M., Tymoczko, J. L., and Stryer, L. (2002) in *Biochemistry*, 5th ed., pp 491−550, Freeman, New York.
20. Bellelli, A., Brunori, M., Brzezinski, P., and Wilson, M. T. (2001) Photochemically induced electron transfer, *Methods 24*, 139−152.
21. Hayashi, T., Takimura, T., and Ogoshi, H. (1995) Photoinduced singlet electron transfer in a complex formed from zinc myoglobin and methyl viologen: Artificial recognition by a chemically modified porphyrin, *J. Am. Chem. Soc. 117*, 11606−11607.
22. Willner, I., Zahavy, E., and Heleg-Shabtai, V. (1995) Eosin-modified reconstituted Co(II) protoporphyrin IX myoglobin: A semisynthetic photoenzyme for H_2 evolution and hydrogenation, *J. Am. Chem. Soc. 117*, 542−543.
23. Hamachi, I., Tanaka, S., Tsukiji, S., Shinkai, S., and Oishi, S. (1998) Design and semisynthesis of photoactive myoglobin bearing ruthenium tris(2,2′-bipyridine) using cofactor-reconstitution, *Inorg. Chem. 37*, 4380−4388.
24. Hu, Y.-Z., Tsukiji, S., Shinkai, S., Oishi, S., and Hamachi, I. (2000) Construction of artificial photosynthetic reaction centers on a protein surface: Vectorial, multistep, and proton-coupled electron transfer for long-lived charge separation, *J. Am. Chem. Soc. 122*, 241−253.
25. Winkler, J. R., and Gray, H. B. (1992) Electron transfer in ruthenium-modified proteins, *Chem. Rev. 92*, 369−379.
26. Gray, H. B., and Winkler, J. R. (1996) Electron transfer in proteins, *Annu. Rev. Biochem. 65*, 537−561.
27. Winkler, J. R., Nocera, D. G., Yocom, K. M., Bordignon, E., and Gray, H. B. (1982) Electron-transfer kinetics of pentaammineruthenium(III)(histidine-33)-ferricytochrome *c*. Measurements of the rate of intramolecular electron transfer between redox centers separated by 15 Å in a protein, *J. Am. Chem. Soc. 104*, 5798−5800.
28. Nocera, D. G., Winkler, J. R., Yocom, K. M., Bordignon, E., and Gray, H. B. (1984) Kinetics of interamolecular electron transfer from Ru^{II} to Fe^{III} in ruthenium-modified cytochrome *c*, *J. Am. Chem. Soc. 106*, 5145−5150.
29. Horton, R. M. (1993) in *Methods in Molecular Biology* (White, B. A., Ed.) pp 251−261, Humana Press, Totowa, NJ.
30. Springer, B. A., and Sligar, S. G. (1987) High-level expression of sperm whale myoglobin in *Escherichia coli*, *Proc. Natl. Acad. Sci. U.S.A. 84*, 8961−8965.
31. Li, T., Quillin, M. L., Phillips, G. N., Jr., and Olson, J. S. (1994) Structural determinants of the stretching frequency of CO bound to myoglobin, *Biochemistry 33*, 1433−1446.
32. Carver, T. E., Brantley, R. E., Jr., Singleton, E. W., Arduini, R. M., Quillin, M. L., Phillips, G. N., Jr., and Olson, J. S. (1992) A novel site-directed mutant of myoglobin with an unusually high O_2 affinity and low autooxidation rate, *J. Biol. Chem. 267*, 14443−14450.
33. Bickar, D., Bonaventura, C., and Bonaventura, J. (1984) Carbon monoxide-driven reduction of ferric heme and heme proteins, *J. Biol. Chem. 259*, 10777−10783.
34. Brzezinski, P., and Malmström, B. G. (1985) The reduction of cytochrome *c* oxidase by carbon monoxide, *FEBS Lett. 187*, 111−114.
35. Marcus, R. A., and Sutin, N. (1985) Electron transfer in chemistry and biology, *Biochim. Biophys. Acta 811*, 265−322.
36. Hopfield, J. J. (1974) Electron transfer between biological molecules by thermally activated tunneling, *Proc. Natl. Acad. Sci. U.S.A. 71*, 3640−3644.
37. Langen, R., Chang, I.-J., Germanas, J. P., Richards, J. H., Winkler, J. R., and Gray, H. B. (1995) Electron tunneling in proteins: Coupling through a β strand, *Science 268*, 1733−1735.

BI0507581